

The mineralogy and geochemistry of Neogene sediments from eastern Turkey, southeast of Arapgir (Malatya)

Dicle BAL AKKOCA*, Zeynep BAYTAŞOĞLU

Department of Geological Engineering, Faculty of Engineering, Fırat University, Elazığ, Turkey

Received: 24.02.2012 • Accepted: 29.11.2012 • Published Online: 13.06.2013 • Printed: 12.07.2013

Abstract: The mineralogy and geochemistry of volcanoclastic sediments in the southeastern part of the Arapgir area (Malatya) were studied by optical microscopy, XRD, SEM, ICP-AES, and MS techniques. Samples were collected from the marine and lacustrine deposits of the Dibekli and Böğürlüdağ sections that contained calcite, clay minerals, feldspar, quartz, dolomite, and opal. Clay minerals were mixed layer smectite-chlorite, illite, and palygorskite, with Ca-smectite being the dominant clay phase. Smectite was derived from the transformation of volcanic glass and volcanic rock fragments. The fact that Y, Sc, Co and Σ REE concentrations and (La/Lu)_N, La/Sc, Sc/Th, Co/Th, Th/U, and Zr/Hf ratios of tuffites of marine and lacustrine formations are quite similar suggests that these deposits had a common source. The marine sediments of the Alibonca Formation under the volcano sedimentary units are derived from Yamadağ volcanic products and, therefore, volcanism might have commenced in the Lower Miocene.

Key words: Yamadağ Volcanics, marine and lacustrine sediments, clay mineralogy

1. Introduction

The effect of volcanism on sedimentary basins and their clay mineral assemblages has been the subject of intense research activity (Christidis *et al.* 1995; Çelik *et al.* 1999; Tandon 2002; Ece & Nakagawa 2003; Shoval 2004; Abdioğlu & Arslan 2005; Yıldız & Kuşcu 2007; Ece *et al.* 2008; Erkoyun & Kadir 2011; Karakaya MÇ *et al.* 2011; Karakaya N *et al.* 2011).

Smectites in volcanic environments are the most important products by means of alteration of volcanic detritus (Yalçın & Gümüşer 2000; Huff 2006; Christidis & Huff 2009). In addition, the mineralogy and geochemistry of smectite-rich sedimentary deposits have increasingly been used as tools for investigating various geological problems due to their higher abundances of trace elements (Taylor & McLennan 1985; Leo *et al.* 2002; Lopez *et al.* 2005). Most of the geochemical research has shown relatively immobile behavior of several trace elements in sedimentary processes, which remain in clays or associated heavy minerals (Lopez *et al.* 2005; Karakaya 2009).

During the Neogene, convergence between Arabian and Anatolian plates developed (Şengör *et al.* 1985; Şaroğlu & Yılmaz 1986). The transgressive sea that covered Eastern Anatolia during the Early Miocene probably resulted from the development of the southeastern arm of the Tethys Ocean, which spread westward and eastward,

depositing shallow marine carbonates and siliciclastics in eastern Turkey. In association with this regime, the Yamadağ Volcanism in the Miocene blanketed almost all of East Anatolia. This volcanism was accompanied by fluvial and lacustrine deposits (Şaroğlu & Yılmaz 1986). The age of Yamadağ Volcanism has been debated. Leo *et al.* (1974) and Ercan and Asutay (1993), based on radiometric age data, proposed that Neogene volcanism was formed in 3 stages starting with the Middle Miocene and ending in the Upper Miocene. Kürüm *et al.* (2006) examined the mineralogy, petrography, and geochemistry of Yamadağ Volcanism in Eski Arapgir. Türkmen *et al.* (1998), who studied the stratigraphy of the Eski Arapgir area, considered intercalation of volcanic volcanoclastics and shallow marine carbonates in the upper levels of the Early Miocene and suggested that the volcanic activity was triggered in the Early Miocene.

Although the stratigraphy of the Alibonca Formation and Yamadağ Volcanic rocks has been studied, there has been no work on the mineralogy and geochemistry of the marine and lacustrine units from this area. This area was chosen because the Alibonca Formation is a part of an enormous sedimentary succession that was deposited during the Mesozoic transgression in East Anatolia. Moreover, the Yamadağ Volcanism is one of the most representative parts of the Neogene Volcanics spread

* Correspondence: dbal@firat.edu.tr

out in East Anatolia in terms of age and tectonic setting. Hence, this study has regional importance.

The aim of this study is to interpret the mineralogical and geochemical characteristics in order to investigate the precipitation mechanisms of smectites in the lacustrine and marine sediments that are syngenetic with the Yamadağ Volcanism; to characterize the distribution of minerals, major, trace, and rare earth elements (REEs) in the marine and lacustrine sediments; and to compare the mineralogical and geochemical characteristics of investigated units. Such a comparison is important in order to ascertain whether the clastics in the Lower Miocene Alibonca Formation are derived from Yamadağ Volcanism, which might reveal the timing of the commencement of volcanism. This is clearly a topic that is of interest not only to the clay science community, but also to the larger community of geoscientists interested in the Neogene history of this region, as well.

2. Geology

The study area is located in the southeastern part of Arapgir (Malatya) in the vicinity of Eski Arapgir and Dibekli, where Permo-Triassic Keban Metamorphics, the Lower Miocene marine Alibonca Formation, the Miocene Yamadağ Volcanics, and intercalated lacustrine rocks comprise the main lithologic units (Figure 1). The reddish metamorphic complex consists of marbles, unconformably overlain by the Alibonca Formation, which was deposited in a turbulent, shallow marine environment (Türkmen *et al.* 1998). In the studied section, the lower part of the Alibonca consists of thick, cream-yellow-colored, fossiliferous and thin to thick bedded carbonated sandy claystones, clayey limestones, clayey-sandy limestones, brown- and red-colored and fine-grained sandy limestones that change at the top to tuffites (Figure 2). Based on the fossil data determined by Perinçek (1979) and Turan (1984), the age of the unit is Lower Miocene. The Alibonca Formation is overlain by Yamadağ Volcanics, which are composed of limestones, sandy limestones, tuffites, basaltic lava flows, coal levels, and yellow-white chert-bearing lacustrine limestones at the top.

Ercan and Asutay (1993) suggested that these volcanics, with an extensive distribution in the eastern and southeastern Anatolian region, were first formed in Malatya in the middle Miocene, then continued in Elazığ, Tunceli, and Bingöl in the Upper Miocene-Lower Pliocene and ended with Diyarbakır volcanites in the Plio-Quaternary. The age, origin, and tectonic evolution of the Neogene Volcanites in and around the Malatya region were studied by Innocenti *et al.* (1976), Şaroğlu and Yılmaz (1986), Alpaslan and Terzioğlu (1996), Buket and Temel (1998), Keskin *et al.* (1998), Yılmaz *et al.* (1998), and Ekici (2003). Yalçın *et al.* (1998) stated that these volcanics in

the north of Hasançelebi are composed of olivine-bearing intermediate rocks of sodic, calc-alkaline to mildly alkaline character. Ekici (2003) also determined that these volcanites around Arguvan are basaltic andesite to dacite in composition with typical calc-alkaline character. Kürüm *et al.* (2006) stated that lava flows alternating with lacustrine deposits have basaltic composition in the study area. The basaltic and andesitic lavas comprising the first stage of volcanism in the region were dated as Middle Miocene while dacitic lavas of the second stage are Middle-Late Miocene in age (Leo *et al.* 1974). The basaltic lavas of the latest stage are of Upper Miocene-Lower Pliocene age (Leo *et al.* 1974). According to Yalçın *et al.* (1998), based on the stratigraphic relations between the Yamadağ Volcanites and underlying lithologies, their age might shift to early Miocene. Likewise, Türkmen *et al.* (1998) pointed out that volcanism in the region probably started in the Lower Miocene. Volcanism started at Early Miocene, because tuffites of the Early Miocene Alibonca Formation have similar mineralogy and geochemistry as the lacustrine sediments that host the Yamadağ Volcanics.

3. Materials and methods

Forty-five samples were collected from Böğürlüdağ and Dibekli stratigraphic sections from the Alibonca Formation and Yamadağ Volcanites (Figures 3a and 3b). Analyzed samples have been classified into 3 groups: the lower member of the Alibonca Formation consisting of marine limestone and sandy carbonated clayey rocks (Akk samples), its upper member representing altered carbonated-clayey tuffs (Alt samples), and the lacustrine formation consisting of a thick layer of altered tuffites with basaltic lava intercalations (Ymt samples).

For petrographic studies, thin sections of 15 representative samples were examined with an optical microscope (Nikon Pol. 400). Bulk mineralogy was determined by X-ray powder diffraction (XRD) (Rigaku DMAXIII) using Ni-filtered Cu K α radiation at 15 kV to 40 mA at the General Directorate of Mineral Research and Exploration (MTA), Ankara. The clay fractions (<2 μ m) for mineralogical investigations were separated by centrifugation after dispersion. The samples were ground slightly prior to clay extraction in order to prevent clastic micas from entering the clay-sized fraction. The peptizing components of the samples (carbonates and organic matter) were removed via acid treatment. The oriented samples of clay minerals were prepared by pipetting the clay suspension and/or smearing the clay mud onto glass slides. The mineralogical compositions of the clay fractions were assessed by X-ray diffraction. For these analyses, samples of specific fractions were solvated with ethylene glycol (EG) at 60 °C for 16 h and subsequently heated to 490 °C for 4 h. The assignment of diffraction maxima was based on the standard JCPDS file. Mineral percentage

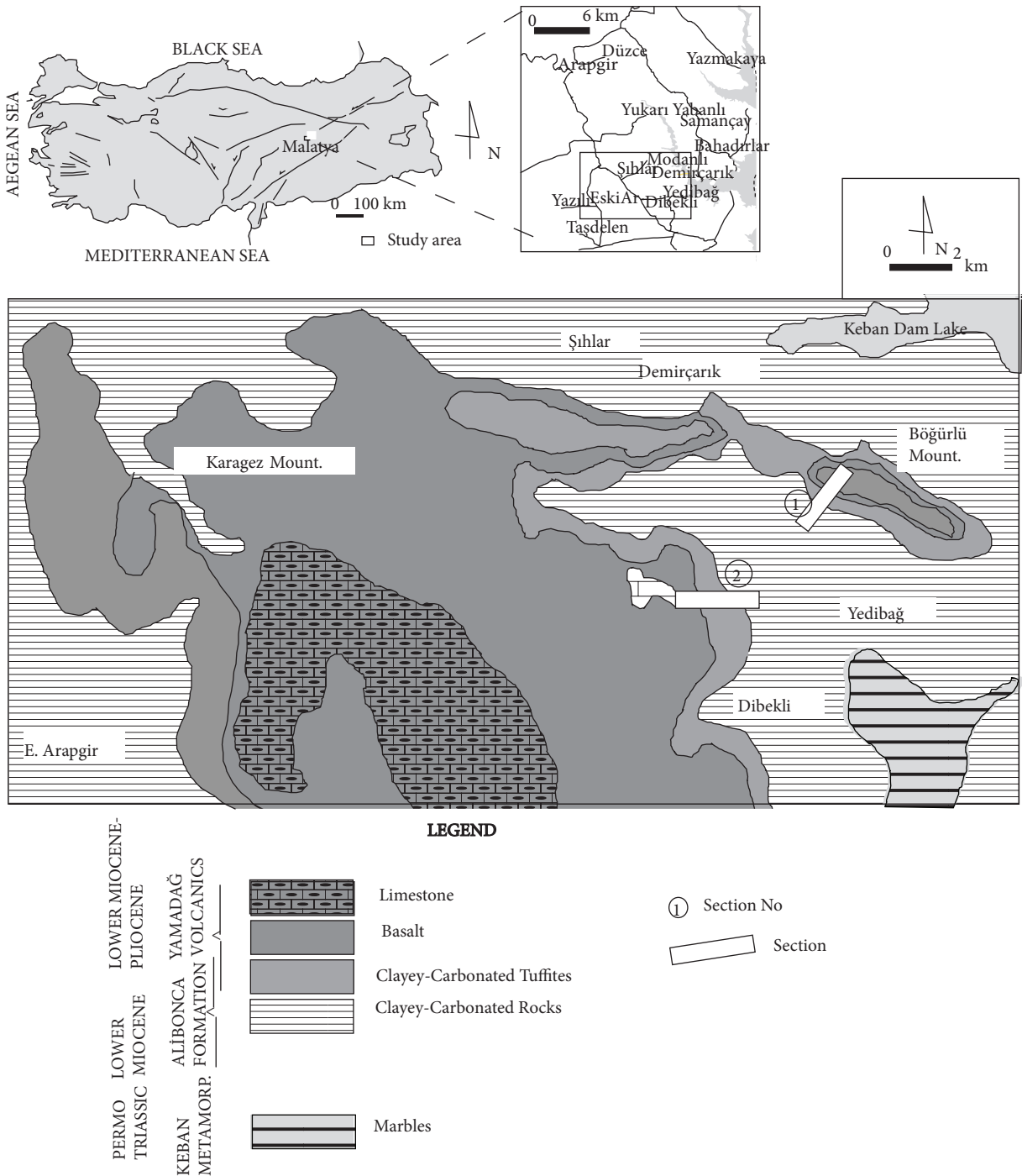


Figure 1. Geological map of study area (simplified from Kürüm 2006).

of whole rock minerals was determined by the technique described by Gündoğdu (1982). In this method, samples were mounted in the same way and the characteristic peak intensities (I) of the minerals were normalized to that of reflection of dolomite. Relative accuracy of this method is within 15%.

An external standard method suggested by Yalçın and Bozkaya (2002), after that of Gündoğdu (1982) and Brindley (1981), was used as a guide for quantitative estimate of clay minerals. Relative abundance of clay minerals was estimated by empirical factors weighting the integrated peak areas of basal reflections. The characteristic

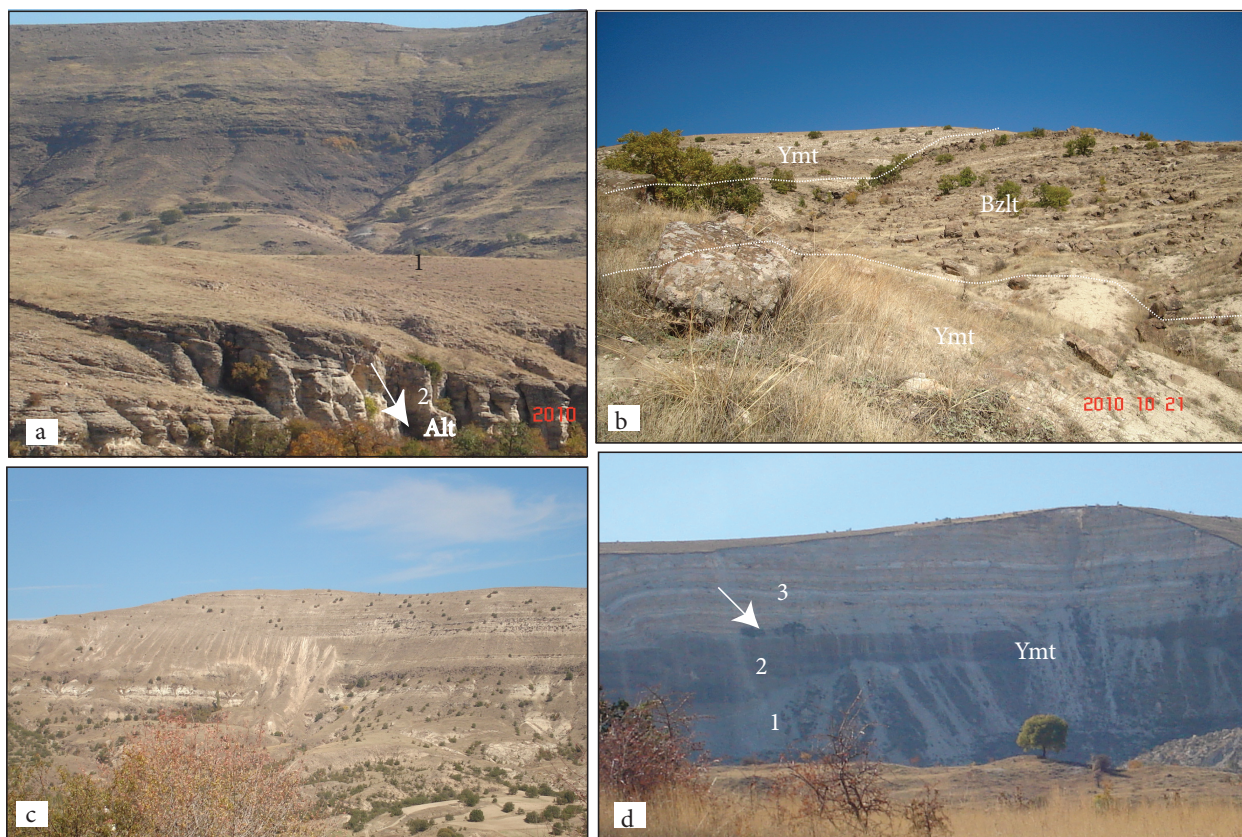


Figure 2. (a) Tuffites from Alt samples. (b-c) Limestone-basalt-tuffite intercalations from Ymt samples, Böğürlüdağ Section. (d) Tuffites (1), basaltic lavas (2), and coal level (arrow) cherty limestones (3) from interbedded lacustrine deposit of Yamadağ Volcanics, behind Böğürlüdağ Section.

peak intensities (I) of the minerals were normalized to that of the reflection of kaolinite. Accordingly, the areas of the glycolated 15-Å peak were multiplied by 1.57 to yield smectite proportions, the area of the 10 peak was multiplied by 1.52 to obtain the illite proportion, the 10.50-Å peak areas were multiplied by 1.46 to estimate palygorskite proportions, and the 7.8-Å peak areas were multiplied by 6.25 to yield mixed layer smectite-chlorite proportions. Relative accuracy of this method is within 15%.

Representative gold-coated, clay-rich freshly broken samples were used for SEM-EDX, analysis with an LO-435 VP scanning electron microscope. Whole rock chemical analyses of 25 representative samples were performed at Acme Analytical Laboratories Ltd. (Canada) using ICP-AES for determination of major and trace elements and ICP-MS for REEs. Chemical analyses of major and trace elements were performed using the following techniques (deduction limits within brackets): major elements (0.1%) and trace elements Y, Ba, Sr (10 ppm), Zr (1 ppm), Rb (2 ppm), and Nb (2 ppm) were analyzed by X-ray fluorescence; Cr (2 ppm), Cs (0.5 ppm), Hf, Th (0.2 ppm),

and U (0.1 ppm) by neutron activation analysis; V (2 ppm), Co, Ni, Sc (1 ppm), and Cu (0.5 ppm) by inductively coupled plasma; and the REEs by inductively coupled plasma mass spectrometry (Eu, Ho, and Lu: 0.05 ppm; the rest of the REEs: 0.1 ppm).

Statistical analyses were carried out using SPSS 8.0. Correlation coefficients were calculated from the data set for the mineralogical and geochemical analyses. Accordingly, the significance level is $\alpha = 0.05$ with correlation coefficient (r) of 0.30. Analysis of variance (ANOVA) was applied to the average La/Yb values of 3 groups of sandy calcareous clayey rocks (Akk samples), altered carbonated-clayey tuffites (Alt samples), and lacustrine formation consisting of thick layer altered tuffites with basaltic lava intercalations (Ymt samples).

4. Results and discussion

4.1. Optical microscopy determinations

The Alibonca Formation is characterized by clay limestones (Akk) with a matrix consisting of calcite and dolomite. Allochems are composed of fossils, while lithoclasts include volcanic and metamorphic rock fragments. Metamorphic

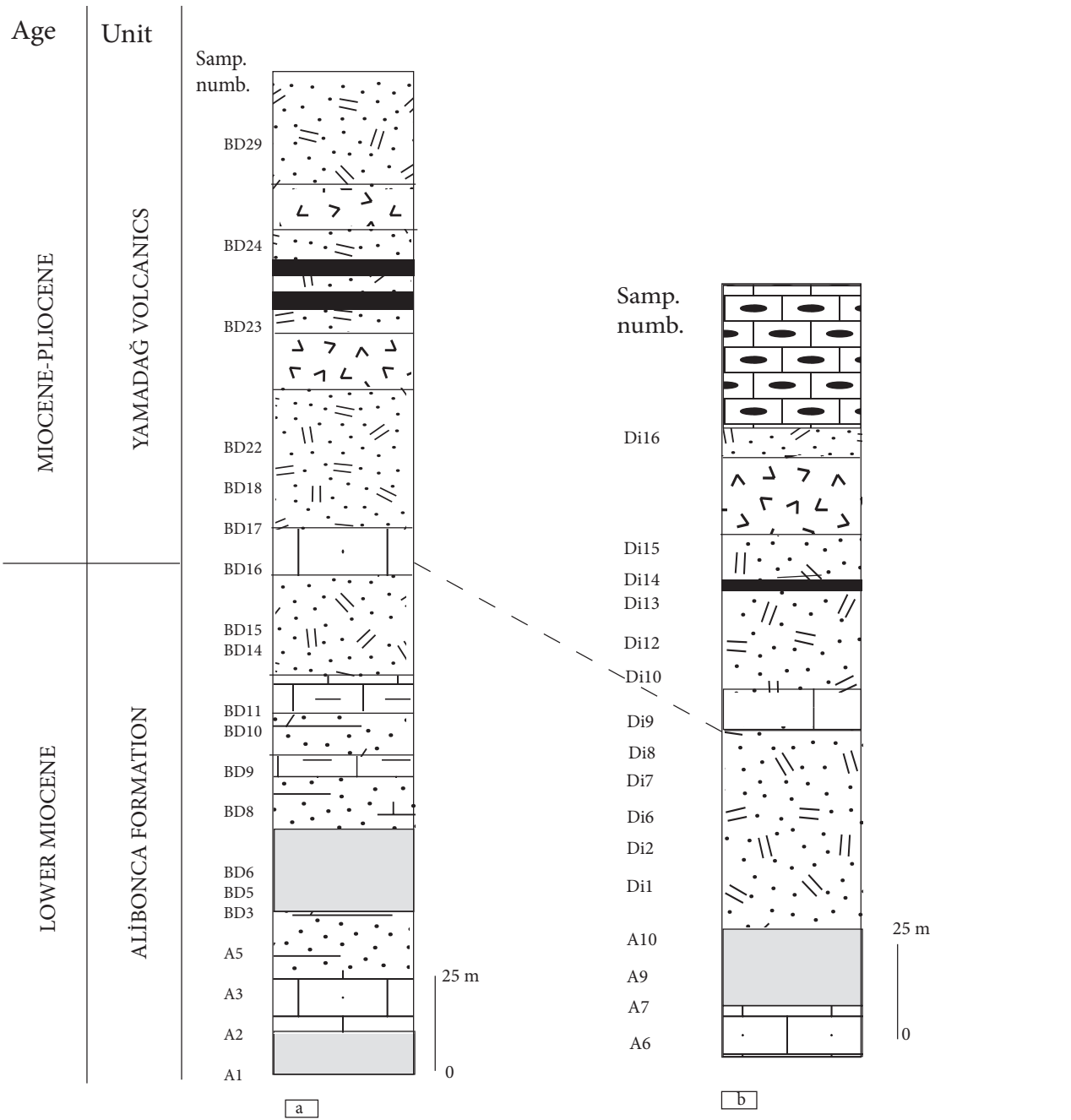


Figure 3. Böğürlüdağ (a) and Dibekli (b) measured stratigraphic sections and sample locations.

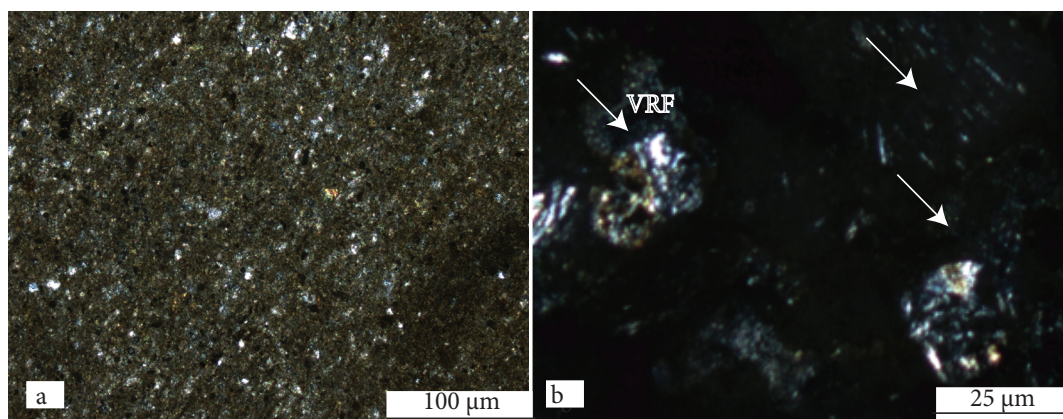


Figure 4. (a) Opaque minerals, argillization, and carbonization in vitric tuffites (Sample No: Di2 sample from Alt). (b) Volcanic rock fragments (VRF) in lithic tuffites (Sample No: BD24 sample from Ymt, crossed light).

rock fragments are absent in the clayey-sandy limestones of the Yamadağ Volcanites.

The volcanic units are composed of volcanic rocks and pyroclastics. Volcanic rocks in the study area have basaltic composition and are composed of plagioclase, clinopyroxene, and olivine and trace amounts of orthopyroxene, chlorite, serpentine, carbonates, and sericite (Kürüm *et al.* 2006).

Alt and Ymt samples are composed of vitric and lithic tuffites. Opaque minerals, argillization, and carbonization are noticeable in the vitric tuffs (Figure 4a). In addition, locally occurring carbonate and volcanic rock fragments are also detected in lithic tuffs. The lithic tuffites of the

lacustrine units also often contain basaltic rock fragments (Figure 4b).

4.2. XRD investigations

Whole rock and clay fraction mineral analyses of the Akk, Alt, and Ymt samples are listed in Table 1. All samples consist of calcite, clay minerals, feldspar, quartz, dolomite, and opal. Trace amounts of pyrite are also present only in Ymt samples.

Clay minerals are composed of smectite, illite, palygorskite, and mixed layers of smectite-chlorite. XRD patterns of air-dried, glycol-treated, and heated samples are shown in Figure 5. Basal reflections on Ca-smectites range between 15.0 and 15.5 Å. After glycol treatment, the

Table 1. Bulk and clay mineralogy percentages of Alibonca marine lower level samples (Akk), Alibonca marine upper level tuffite samples (Alt), and Yamadağ Volcanics samples (Ymt). Max: maximum, Min: minimum, n: sample number, SD: standard deviation.

Bulk mineralogy	Akk samples (n = 15)				Alt samples (n = 8)				Ymt samples (n = 13)			
	Mean	Max.	Min.	SD	Mean	Max.	Min.	SD	Mean	Max.	Min.	SD
Clay	32	53	11	11.97	38	47	26	7.17	33	49	11	12.35
Feldspar	10	32	1	10.16	28	51	12	13.03	36	60	13	17.16
Quartz	7	16	2	4.68	4	6	3	1.06	3	5	1	1.44
Calcite	59	95	24	20.35	24	37	9	10.28	21	44	3	11.09
Dolomite	5	11	2	2.59	5	11	1	3.37	7	16	2	4.60
Opal	4	4	4	...	9	12	5	3.78	7	13	2	4.16

Clay mineralogy	Akk samples (n = 12)				Alt samples (n = 8)				Ymt samples (n = 12)			
	Mean	Max.	Min.	SD	Mean	Max.	Min.	SD	Mean	Max.	Min.	SD
Smectite	66	100	32	19.76	71	90	68	8.01	80	91	65	7.87
Illite	14	26	3	10.35	6	11	3	3.46	5	13	2	4.76
Palygorskite	24	50	3	15.97	16	25	7	6.76	14	25	6	6.17
Smectite-chlorite	16	25	5	8.01	8	15	4	4.99	11	25	2	8.73

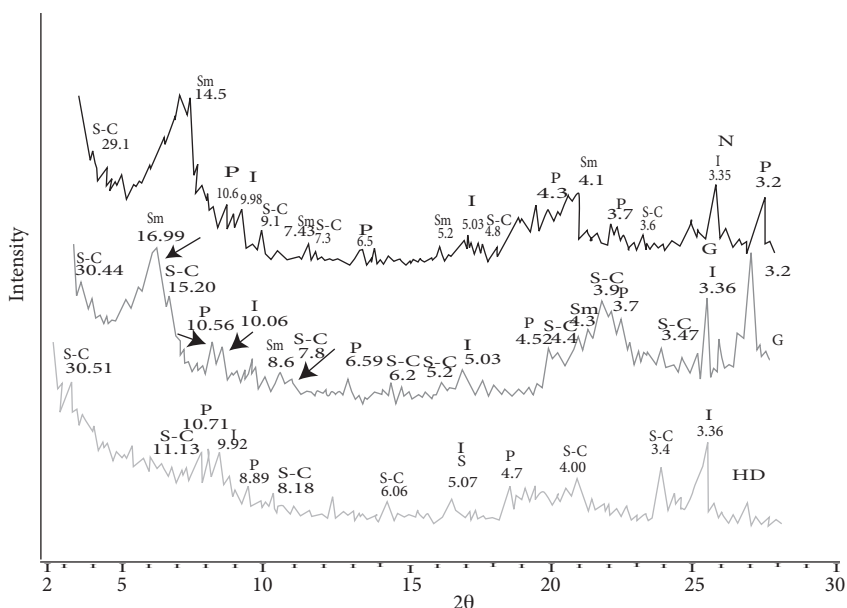


Figure 5. X-ray diffractogram of representative clay fraction of BD8 samples. S: smectite, I: illite, S-C: smectite-chlorite, P: palygorskite. The characteristic peak intensities (I) (arrow) of each minerals were normalized to that of the reflection of kaolinite for semi-quantitative analyses according to Yalçın and Bozkaya (2002) after Gündoğdu (1982) and Brindley (1981). Relative accuracy of this method is within 15%.

XRD patterns revealed basal spacing of 17 Å (001), 8.6 Å (002), and 4.3 Å (004) for the Ca smectites. Typical XRD patterns showed that the (001) peak at about 10 Å for illite, (001) peak at about 29 Å for S-C, and (001) peak at about 10.6 Å for palygorskite are represented for air-dried samples (Figure 5).

Whole rock and clay distributions of the studied sections are shown in Figures 6a and 6b. Akk samples contain calcite, clay minerals, feldspar, quartz, dolomite, and opal. Alt and Ymt samples consist of clays, feldspar, calcite, opal, dolomite, and quartz. Carbonated clayey samples (Akk) are rich in calcite. Tuffites contain much more feldspar than Akk samples. The abundance of clay minerals in the 3 groups' samples are almost similar and consist of smectite, palygorskite, smectite-chlorite, and illite, respectively (Table 1; Figure 6).

4.3. SEM observations

In sample A6, most of the calcite crystals are euhedral (rhombic) and subeuhedral (Figure 7a), with a spherical or rounded appearance (Figure 7b), and are smaller than 10 µm in diameter.

Similar results were obtained under SEM for the Di6 (Alt) and BD23 (Ymt) samples. Authigenic smectites are important components in all tuffite samples. Smectites replace volcanic glass, volcanic fragments, and intergranular pores (Figure 8a); they are usually wavy and flaky and often yield characteristic honeycomb textures (Figure 8b). Likewise, Christidis (2001) described the

smectite forms first during dissolution of the volcanic glass through nucleation and crystal growth, leading to pseudomorphic textures after volcanic glass.

5. Geochemistry and statistical analysis

5.1. Major and trace elements

Smectite-rich rocks are widely used for determining the geochemical affinities of the magmatic component (Plank & Langmuir 1998; Spears *et al.* 1999; Worash & Valera 2002). Major and trace element concentrations of the studied samples are listed in Table 2.

Volcanic samples of Kürüm *et al.* (2006) and the sediment samples of the present study in the discrimination diagram of Winchester and Floyd (1977) indicate subalkaline basalt composition for the volcanic rocks; 6 samples are subalkaline basalt and the others are of andesitic composition for the marine and lacustrine sediments (Figure 9).

Samples A2 and A3 have high carbonate and CaO contents. MgO concentration was high in sample B22, which contained basaltic rock fragments (Table 2). A linear regression and correlation analysis (confidence level = 0.95) was performed to reveal any communality of minerals and elements. Some correlation plots for major and trace elements are shown in Figure 10.

SiO₂ is positively correlated with Al₂O₃, Na₂O, and TiO₂ ($r = 0.53-0.93$) and negatively correlated with CaO ($r = -0.95$). This suggests that CaO is derived primarily from

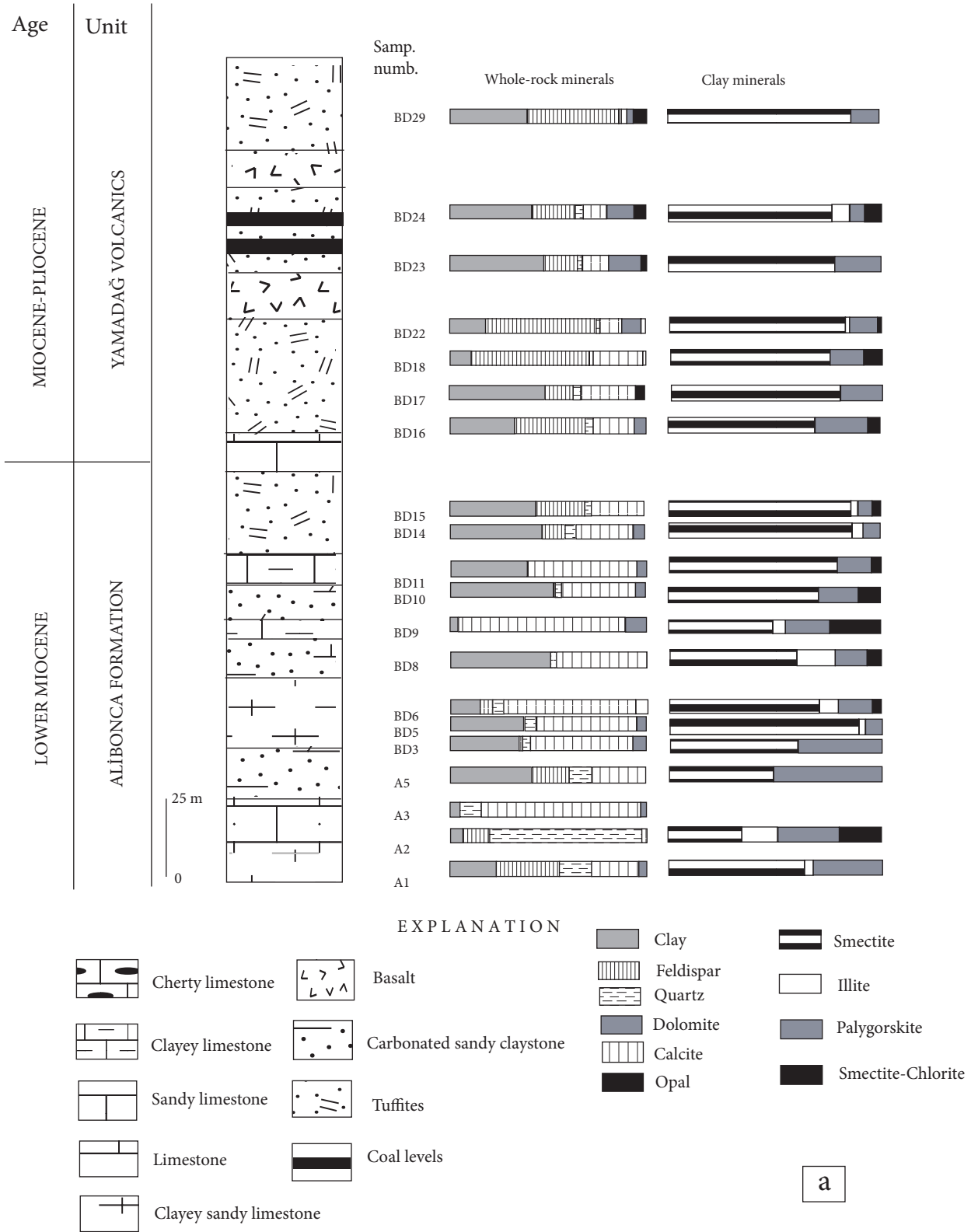


Figure 6. Whole rock and clay distributions of (a) Bögürlüdağ and (b) Dibekli sections.

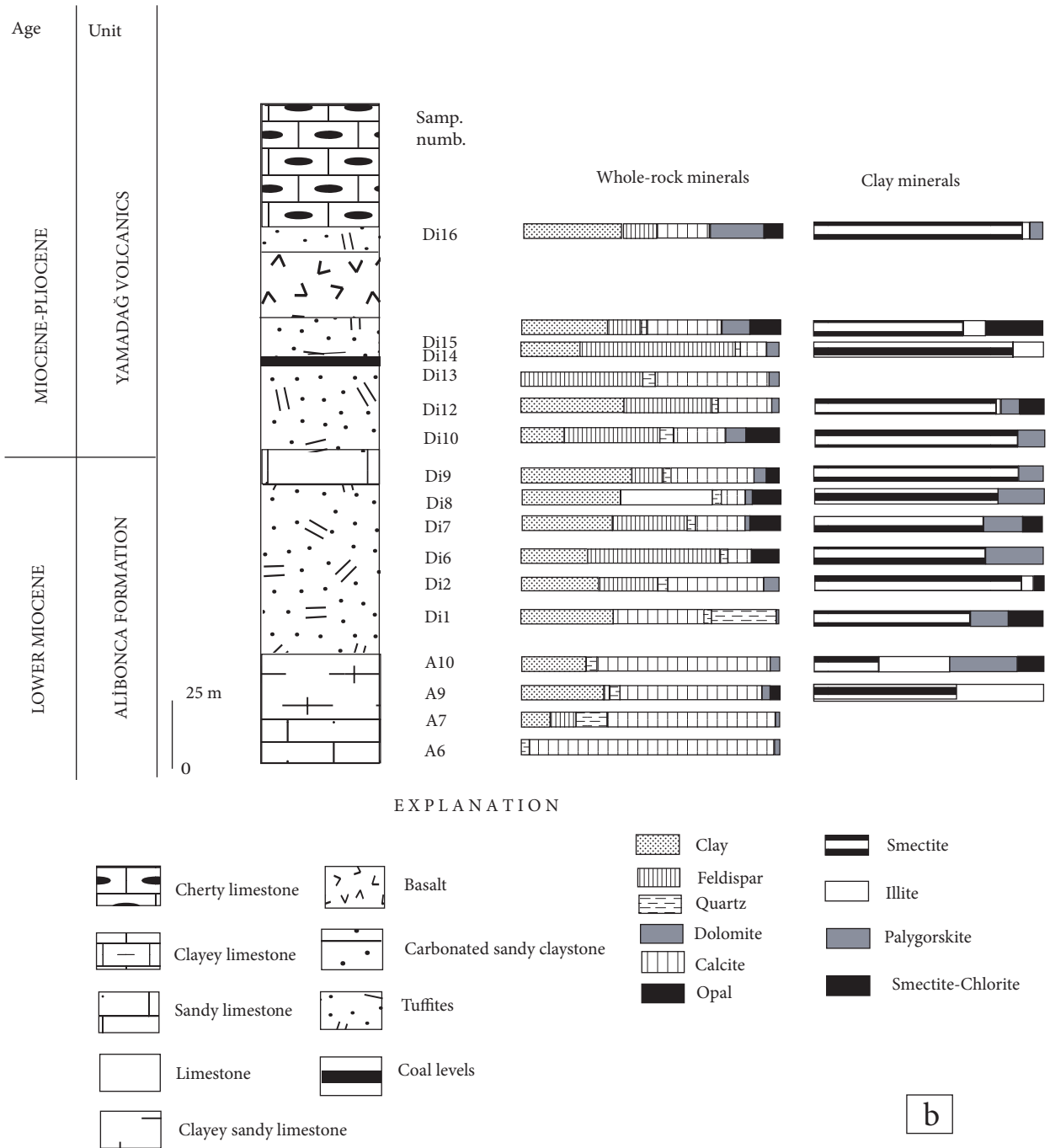


Figure 6 continued

carbonates, but other elements are associated with silicates. Rb is positively correlated with K_2O ($r = 0.85$), indicating that a similar geochemical behavior is associated with feldspar and illite since both elements are preferentially retained in illite during weathering (Das & Haake 2003). Positive correlations between Ti and Sc, Co, and V ($r > 0.80$), and between Nb and Ta and Th ($r > 0.70$), suggest that Ti- and Nb-bearing minerals may at least partially

control the distribution of certain trace elements (Lopez *et al.* 2005). Rashid (2002) suggested that aluminum is the main constituent of clay minerals, and positive correlations between Al and Ga (0.99) show that these elements are concentrated in phyllosilicates and there is high positive correlation between TiO_2 and Al_2O_3 ($r = 0.95$), indicating that Ti exists primarily in the clay fraction. The poor and absent correlations between Al and the Ni, Cu, and Pb

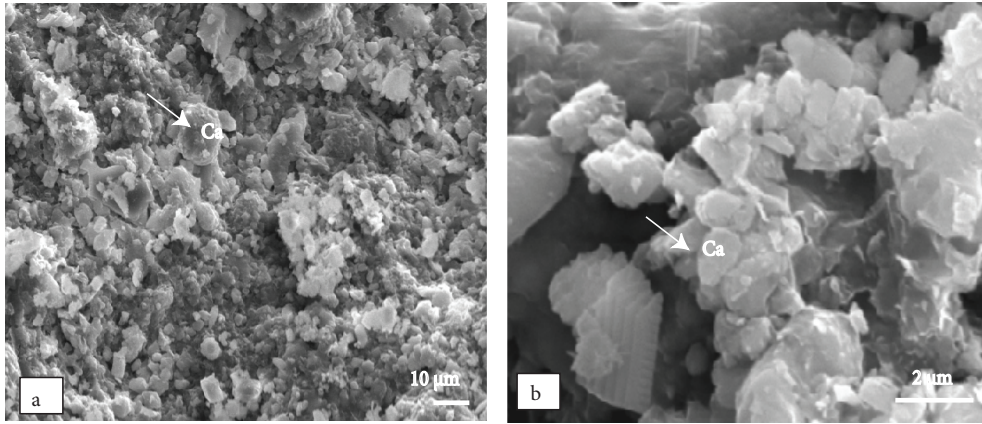


Figure 7. SEM pictures of carbonate muds. (a-b) Mosaic of euheral (rhombic) and subeuheral calcite crystals (Ca), with a spherical or rounded habit and variable size and shape (A6: Akk samples).

elements ($r = -0.39$ to 0.15) suggest that these elements may be associated with mafic and opaque phases. This is also shown by moderately positive correlations between Cu and Ni ($r = 0.54$) and Zn ($r = 0.81$). Positive correlations

between Cu and Fe ($r = 0.94$) and Ti ($r = 0.85$) indicate basaltic rock fragments in samples. Moreover, the positive correlations between Fe_2O_3 and Sc, V, TiO_2 , and Co ($r = 0.86-0.96$) indicate mafic hosts (Saleemi & Ahmed 2000).

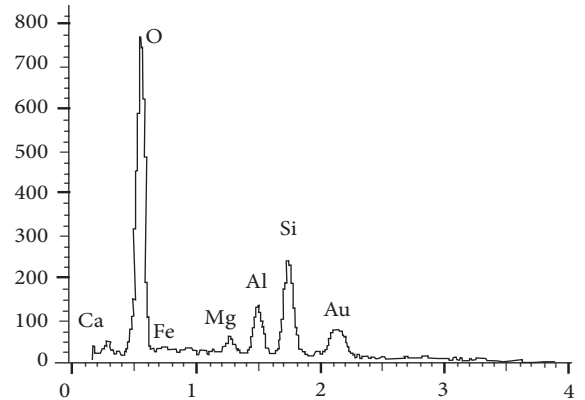
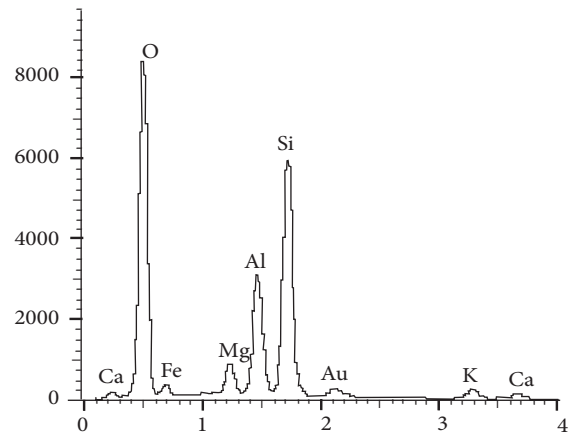
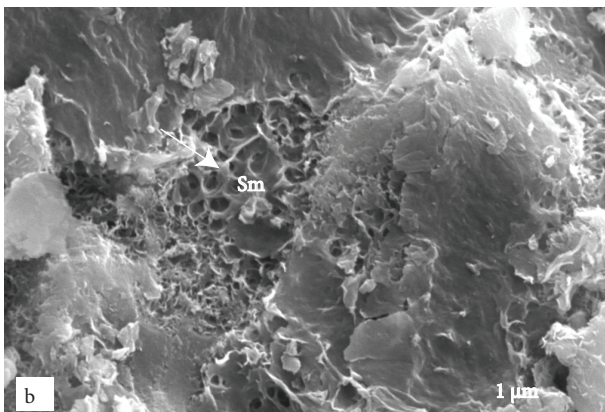
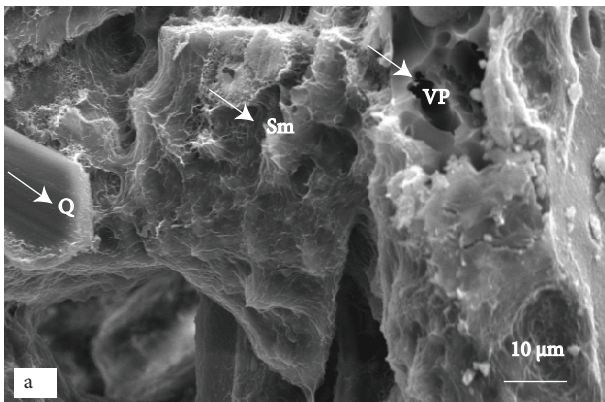


Figure 8. SEM and EDX spectra from (a) authigenic smectites (Sm) replacing volcanic glass (VP), Q: Quartz (BD23: Mlt samples); (b) dissolution of honeycomb fabric, formed by smectite (Di 6: Alt samples).

Table 2. Major and trace element contents of Alibonca lower level samples (Akk), Alibonca upper level tuffite samples (Alt), and Yamadağ Volcanics samples (Ymt).

		Concentration (wt.%)												
	Sample no.	SiO ₂	Al ₂ O ₃	Fe ₂ O ₃	MgO	CaO	Na ₂ O	K ₂ O	TiO ₂	P ₂ O ₅	MnO	Cr ₂ O	LOI	Total
Akk	A1	36.76	9.55	4.88	2.64	20.05	0.33	1.49	0.5	0.06	0.06	0.032	23.5	99.86
	A2	26.52	5.71	2.82	1.50	31.79	0.54	0.71	0.32	0.05	0.17	0.026	29.7	99.90
	A3	28.72	5.67	2.57	1.36	31.18	0.65	0.67	0.29	0.04	0.16	0.025	28.6	99.91
	A5	44.07	10.85	5.33	3.50	13.66	0.2	1.9	0.58	0.05	0.06	0.04	19.6	99.83
	A7	27.38	6.97	3.05	2.15	28.66	0.40	0.91	0.32	0.07	0.12	0.03	29.8	99.82
	BD8	30.0	8.14	4.39	3.87	23.96	0.47	1.21	0.44	0.10	0.06	0.031	27.1	99.81
	BD11	26.56	7.32	4.46	4.21	25.9	0.21	1.35	0.37	0.10	0.05	0.03	29.2	99.77
	DI1	38.33	10.72	2.84	3.16	19.68	1.40	0.82	0.44	0.07	0.04	0.022	22.3	99.85
Alt	DI2	31.99	9.42	2.40	2.15	26.01	1.59	0.81	0.34	0.07	0.02	0.014	25.0	99.85
	DI6	56.42	19.71	3.58	2.15	6.21	4.27	1.26	0.54	0.09	0.03	0.011	5.6	99.85
	DI7	52.24	15.94	3.84	2.75	9.41	3.04	1.34	0.65	0.12	0.03	0.022	10.4	99.83
	DI8	42.33	12.15	4.00	2.92	15.89	1.7	1.25	0.52	0.09	0.05	0.023	18.9	99.85
	DI9	36.69	9.17	3.85	2.79	21.23	0.97	1.21	0.42	0.08	0.05	0.021	23.4	99.86
	BD14	40.94	9.91	3.8	4.35	16.08	0.78	1.46	0.39	0.11	0.06	0.042	21.9	99.80
	BD15	43.81	10.99	3.79	4.15	14.32	1.00	1.27	0.47	0.11	0.05	0.03	19.8	99.80
	DI12	44.46	13.83	3.4	2.37	15.9	2.60	1.08	0.48	0.10	0.03	0.023	15.6	99.84
	DI13	37.47	13.15	1.71	1.03	23.89	3.29	0.61	0.26	0.05	0.13	0.009	18.3	99.88
	DI15	36.21	10.93	3.32	4.34	19.54	1.82	1.08	0.43	0.07	0.05	0.012	22.0	99.78
	DI18	51.67	17.14	4.17	3.11	9.00	3.49	1.19	0.64	0.10	0.04	0.015	9.2	99.81
Ymt	BD17	38.83	9.54	3.43	3.78	18.69	1.14	1.15	0.44	0.09	0.06	0.033	22.6	99.83
	BD19	39.3	11	2.56	2.05	21.53	2.33	0.91	0.35	0.06	0.09	0.027	19.6	99.85
	BD22	40.23	10.76	4.46	6.35	13.71	1.00	1.52	0.49	0.08	0.08	0.021	21.1	99.76
	BD23	37.9	11.93	2.98	4.55	18.44	2.29	1.03	0.41	0.07	0.09	0.021	20.1	99.78
	BD24	47.0	15.86	8.46	3.19	7.02	2.13	1.19	1.27	0.15	0.04	0.036	13.5	99.84
	BD29	47.84	14.23	10.29	2.33	8.84	2.16	0.51	1.27	0.14	0.06	0.034	12.1	99.86

Table 2 continued

Sample		Concentration (ppm)									
		Sc	Ba	Co	Cs	Ga	Hf	Nb	Rb	Sr	Ta
Akk	A1	13	217	18.8	3.3	10.3	2.5	8.3	53.4	290	0.7
	A2	8	161	12.4	1.4	5.9	1.9	4	23.1	311.1	0.2
	A3	8	126	10.9	1.3	5.5	1.9	4.1	20.5	302.8	0.2
	A5	13	367	20.5	4	11.8	2.9	9.6	66.3	257.5	0.7
	A7	7	645	15	2.2	6.7	2	6	30.7	374.8	0.4
	BD8	11	153	18.5	3.4	8.8	1.8	6.2	42.8	699.6	0.4
	BD11	11	224	17	3.6	7.8	1.8	6.1	43.9	882.1	0.4
	DI1	8	169	12.1	3.9	11.3	1.7	5.2	45.9	506.2	0.4
Alt	DI2	7	176	7.1	2.6	10.2	1.7	4.5	29.8	667.8	0.3
	DI6	9	229	10.4	3	20.9	3.1	6.2	54.5	648.7	0.5
	DI7	10	268	11	6	16.3	4.3	7.1	78.5	610.5	0.6
	DI8	10	171	12.3	3.6	12.6	2.4	6.1	51.8	479.6	0.5
	DI9	10	163	11.9	3.3	10.9	2	5.2	47	446.8	0.5
	BD14	10	297	13.7	4.5	9.8	2.7	6.5	58.5	545.3	0.5
	BD15	9	224	15.7	4.3	11.6	2.7	6.9	54.9	670.4	0.7
	DI12	9	201	10.1	2.9	15.3	2.8	5.7	43.1	615.1	0.5
	DI13	5	159	4.4	0.9	13.2	1.1	2.8	15.3	681.9	0.2
	DI15	8	206	10.9	3	11.9	2.1	5.1	44.4	925.1	0.4
	DI18	11	236	12	3	19.4	3	6.7	45.8	748.7	0.5
Ymt	BD17	9	204	14.2	4	10.3	2.6	5.8	48.5	543.3	0.6
	BD19	7	214	8	2	10.5	1.9	4	32.8	605.9	0.3
	BD22	11	192	16.8	4.3	12.1	2.2	6.2	65.9	771.9	0.6
	BD23	8	218	11.6	2.4	12.8	1.8	4.5	37	896.8	0.4
	BD24	28	182	40.1	1.7	16.1	3.1	6.8	33.7	373.2	0.5
	BD29	24	118	30.3	7.9	15.5	2.8	5.7	24.5	385.9	0.4

Table 2 continued

Sample no.		Concentration (ppm)									
		Th	U	V	W	Zr	Y	Cu	Pb	Zn	Ni
Akk	A1	5.2	1.4	98	1	90.1	16.9	26.2	9.6	52	141.3
	A2	3	0.8	64	0.6	65	15.4	15.7	6.1	30	76.6
	A3	2.2	0.8	58	0.5	59.6	14.9	15.6	5.8	28	65.9
	A5	6.9	1.3	107	1.1	105.8	16.6	26.3	11.4	55	168.0
	A7	4.4	1.1	45	0.7	73.6	11.6	12.5	5.6	25	109.6
	BD8	3.8	1.7	79	0.7	68.2	12.3	26.7	9.5	59	176.7
	BD11	3.8	2	94	0.7	64.9	12.1	14.4	8	56	190.4
	DI1	5.2	1.1	61	0.6	66.8	10	8.9	7.5	27	54.6
Alt	DI2	4.3	1.3	41	0.6	62.4	8.6	11.8	5.5	28	38.4
	DI6	5.2	0.8	51	0.5	103.8	9.2	12	5.8	37	41.4
	DI7	6.7	1.3	68	0.9	148.6	10.7	11.4	7.6	35	46.9
	DI8	5.5	1.1	70	1.0	92.2	12.8	13.6	8.8	41	73.1
	DI9	4.8	1	68	1.1	63.3	12.5	12.4	6.3	39	77.8
	BD14	5.7	1.7	61	1.0	95.6	13.7	17.4	9.7	47	109.9
	BD15	7.2	1.6	84	0.9	97.8	12.5	15.7	10.8	42	79.8
	DI12	4.9	1.5	56	0.5	107	12	13	7.4	38	53.3
Ymt	DI13	1.4	4.7	32	0.5	42.8	11.4	6.4	3.6	16	18.4
	DI15	3.8	1.5	59	0.7	69.7	11.8	12.7	6.4	38	54.6
	DI18	5.0	1.3	76	0.5	115.6	11.6	14.7	7.0	41	47.0
	BD17	6.8	1.5	66	0.8	77.5	12.2	14.6	11.5	42	84.6
	BD19	4.0	0.9	48	0.5	72.7	12.8	9.8	10.0	26	52.2
	BD22	6.0	1.7	73	0.9	76.6	12.7	19.7	10.4	48	101.6
	BD23	3.2	1.4	56	0.5	66.6	10.6	13.1	6.8	32	54.4
	BD24	4.0	3.3	182	0.9	112.3	16.6	45.4	5.6	43	87.3
BD29	2.3	1.1	117	0.5	108.3	17.6	48.2	4.0	66	141.6	

5.2. Rare earth elements

REE concentrations of the 3 sample groups are shown in Table 3. Some important correlations between major and trace elements and REEs are shown in Figure 11.

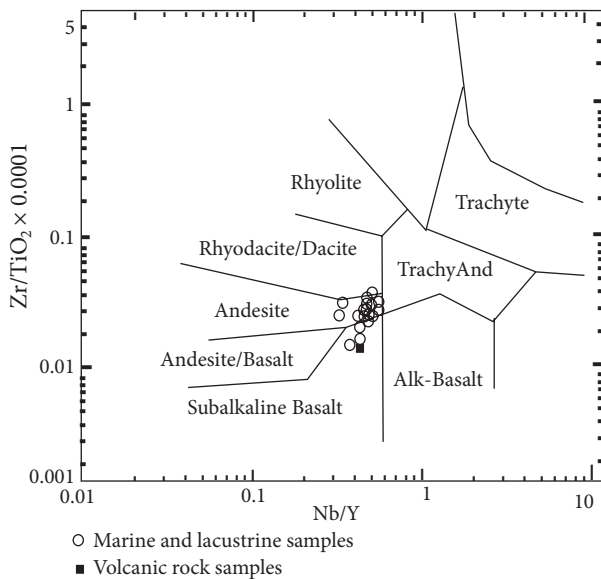


Figure 9. Classification of the marine and lacustrine samples (this study) and volcanic rocks (average values from Kürüm *et al.* 2006) from the study area, based on immobile elements (Winchester & Floyd 1977).

The REEs show a uniform geochemical behavior during any given alteration history (Nesbitt 1979; Kamineni 1985; Middelburg *et al.* 1988). During the alteration of volcanic rocks, soluble REEs migrate from the volcanic glass, whereas their insoluble components tend to be enriched residually in the accessory minerals (Christidis 1998). Accessory minerals, which are not dissolved during weathering, result in residual enrichment of the REEs during formation of clay minerals from glass (Christidis 1998). This is supported by high positive correlation between ΣREE and Nb (0.72) and high positive correlation between ΣHREE and Fe_2O_3 and TiO_2 ($r = 0.78$ and $r = 0.74$, respectively). The high positive correlation between Y and ΣHREE ($r = 0.89$) is due to high geochemical affinity among these elements. High positive correlation in samples between Y and ΣHREE ($r = 0.89$) is attributed to high geochemical affinity among these elements (Lopez *et al.* 2005).

A chondrite-normalized (Sun & McDonough 1989) REE diagram for all Akk, Alt, and Ymt is given in Figure 12. The presence of REE-bearing accessory minerals resulted in a positive LREE anomaly with respect to chondrite (Mongelli 1997). The REE patterns have also been used to infer sources of sedimentary rocks. Chondrite-normalized REEs show no major difference among all the volcanic rocks (Figure 12). Eu/Eu^* are between 0.19 and 0.53 in Akk,

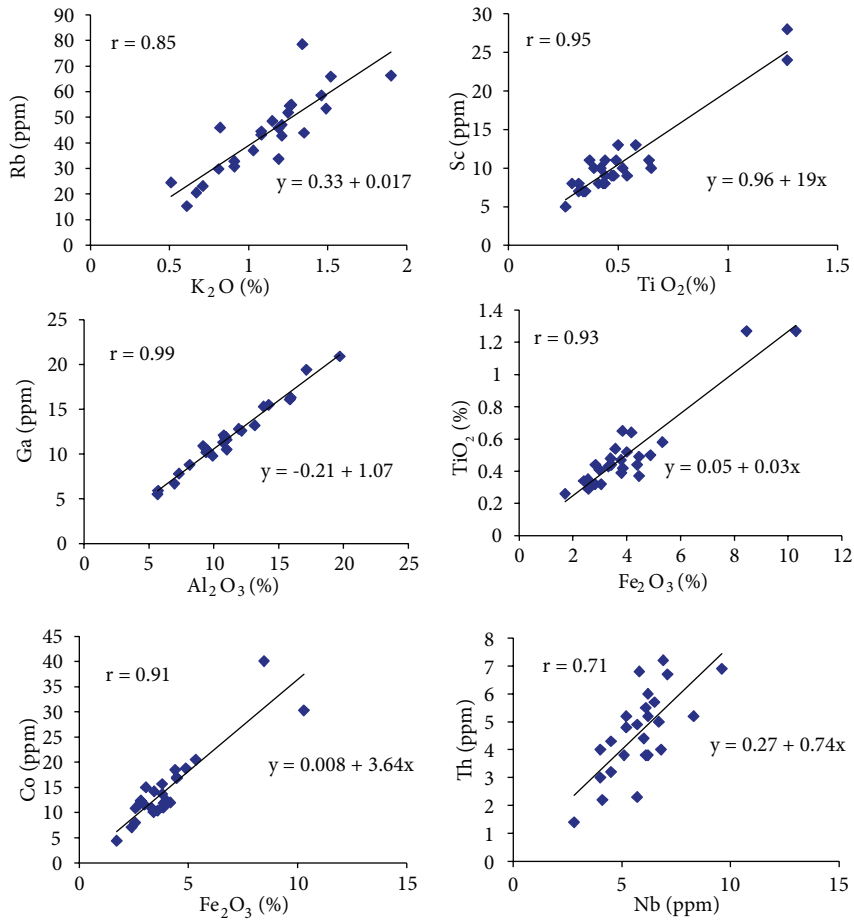


Figure 10. Some representative correlations between major and trace elements (the significance level is $\alpha = 0.05$ for correlation coefficient r).

between 0.23 and 0.40 in Alt, and between 0.20 and 0.53 in Ymt samples. Although most of the studied samples are andesites and basalt in the Winchester and Floyd diagram, Eu/Eu* does not comply with the andesites, which have negative Eu/Eu* = 0.66 (Condie 1993). The Eu anomaly is small at Eu/Eu* = 0.54 in the early stage of the water–basalt interaction, and it increases with interaction time to a final value of about 0.35. In the interaction between rock and water, the negative Eu anomaly seen in the REE pattern increased with leaching time, suggesting that the REEs released in the early stage of weathering mainly originated from minor phases such as some accessory minerals and grain boundary glass, rather than from the more major plagioclase phase (Shibata *et al.* 2006).

5.3. Origin of smectite and sulfur minerals

Volcanic rocks in the study area were described as subalkaline basalt (Kürüm *et al.* 2006). However, marine and lacustrine sediment samples plot in the andesite, lesser subalkaline basalt field of Winchester and Floyd's diagram (1977), indicating that the source rocks may have andesitic composition, although alteration of basaltic rock fragment

is also plausible. Volcanites and pyroclastics around Arguvan about 15 km southwest of the study area are of basaltic andesite to dacite composition (Ekici 2003; Ekici *et al.* 2009) and show a typical calc-alkaline character. Weathering of basaltic and andesitic volcanic material has been shown to yield particularly smectitic clays (Glassman 1982; Ortega-Huertas *et al.* 2002; Hover & Ashley 2003). Clays in the marine and lacustrine sediments may be authigenic through volcanism, halmyrolysis, or early diagenesis (Chamley 1989; Velde 1995). The upper levels of Alibonca (Alt samples) and clays in lacustrine deposits (Ymt samples) were probably derived from the Yamadağ Volcanites through in situ alteration of the source material. SEM observations indicate that honeycomb structure and authigenic smectite clays are important constituents in all samples. The honeycomb shape of the smectite (as shown in Figure 8b) suggests an in situ origin, which is common in sediments (Huggenberg & Fuchtbauer 1988). Among the igneous components, Si, Al, Fe, and K, which were released from the alteration of volcanic glass during diagenesis, were used in the formation of smectites.

Table 3. REE contents of Alibonca lower level samples (Akk), Alibonca marine upper level tuffite samples (Alt), and Yamadağ Volcanics samples (Ymt).

Samp.	Concentration (ppm)														
	La	Ce	Pr	Nd	Sm	Eu	Gd	Tb	Dy	Ho	Er	Tm	Yb	Lu	
Akk	A1	16.3	32.5	3.86	15.2	2.86	0.76	2.99	0.51	2.9	0.61	1.67	0.26	1.72	0.25
	A2	11.2	22.8	2.70	11.1	2.35	0.62	2.4	0.44	2.37	0.51	1.48	0.22	1.47	0.27
	A3	10.2	21.7	2.53	10.7	2.09	0.58	2.34	0.41	2.39	0.49	1.44	0.23	1.43	0.23
	A5	16.9	34.5	4.0	14.9	3.1	0.75	2.68	0.48	2.77	0.56	1.71	0.27	1.64	0.22
	A7	13.4	27	2.95	11.9	2.0	0.6	1.93	0.32	1.73	0.36	1.15	0.17	1.09	0.17
	BD8	11.4	22.8	2.66	10.9	2.07	0.57	1.96	0.35	1.94	0.41	1.14	0.18	1.15	0.17
	BD11	11.7	22.2	2.6	10.2	1.92	0.49	1.92	0.33	1.88	0.38	1.11	0.17	1.07	0.17
Alt	DI1	14.4	28.7	3.21	12.5	2.34	0.75	2.2	0.35	1.83	0.33	0.97	0.16	0.94	0.21
	DI2	10.9	22.7	2.6	10.0	1.95	0.68	1.85	0.29	1.59	0.3	0.83	0.12	0.76	0.17
	DI6	14.6	30.4	3.46	14.3	2.84	1.32	2.54	0.4	2.11	0.35	1.01	0.14	0.83	0.18
	DI7	15.3	32.8	3.77	15.1	3.09	1.08	2.79	0.41	2.19	0.4	1.1	0.16	0.96	0.16
	DI8	14.7	31	3.49	13.8	2.73	0.87	2.62	0.41	2.3	0.45	1.25	0.2	1.25	0.18
	DI9	12.9	27.5	3.05	12	2.46	0.7	2.43	0.39	2.14	0.44	1.3	0.19	1.21	0.14
	BD14	12.8	24.5	2.97	10.7	2.28	0.66	2.28	0.4	2.17	0.47	1.37	0.21	1.35	0.29
	BD15	13.5	28.8	3.21	12.4	2.37	0.63	2.19	0.38	1.97	0.41	1.22	0.17	1.16	0.25
Ymt	DI12	14.3	30.4	3.39	13.3	2.72	1.01	2.54	0.41	2.22	0.43	1.19	0.18	1.10	0.14
	DI13	11.7	21.5	2.34	8.8	1.92	1.01	2.03	0.34	1.90	0.38	1.11	0.17	1.10	0.11
	DI15	13.5	25.5	3	11.3	2.38	0.84	2.31	0.38	2.07	0.42	1.16	0.17	1.10	0.13
	DI18	15.7	35.1	3.88	16.1	3.34	1.29	2.94	0.45	2.46	0.45	1.22	0.18	1.08	0.15
	BD17	14.3	28.9	3.21	13	2.42	0.64	2.18	0.37	1.99	0.39	1.19	0.18	1.13	0.18
	BD19	15.0	27.8	3.17	11.8	2.29	0.82	2.28	0.37	2.02	0.41	1.16	0.18	1.08	0.18
	BD22	15.5	34.2	3.65	14.1	2.64	0.68	2.48	0.41	2.2	0.42	1.23	0.18	1.19	0.16
	BD23	12.6	24.3	2.75	10.8	2.14	0.86	2.19	0.34	1.90	0.37	0.98	0.16	0.91	0.17
	BD24	13.8	33.1	3.51	15.1	3.04	1.12	3.11	0.56	3.22	0.67	1.91	0.29	1.85	0.17
	BD29	8.8	24.1	2.61	11.5	2.69	1.04	3.11	0.54	3.29	0.64	1.77	0.28	1.65	0.16

Pyrite is a common mineral in coal-bearing lacustrine sediments (Křibek *et al.* 1998). Pyrite was detected only in the upper levels of lacustrine samples. Diagenetic pyrite, which is observed in coal veins and/or organic-rich layers, is formed under intermediate-acidic and reducing conditions. The oxidation of soluble Ce^{+3} to the insoluble Ce^{+4} is responsible for the negative Ce anomaly in water (Debaar *et al.* 1985). There are no negative Ce anomalies in the samples (Figure 12), which show reducing conditions. High concentrations of reduced iron and hydrogen sulfide result in formation of iron monosulfides and pyrite in the anoxic water.

5.4. Element distribution of sediments

Na, Mg, K, Sr, and Ca display strong fractionation in marine or lacustrine environments and are mobile during

sedimentary processes (Dalai *et al.* 2004). Therefore, they provide limited information on the source rock characteristics. In contrast, geochemical research has shown that the REEs Y, Sc, Cr, Th, Sc, and Co are relatively immobile in sedimentary processes (Nance & Taylor 1976; Lopez *et al.* 2005), and therefore they are useful for provenance characterization. These elements are believed to be transported exclusively in terrigenous components of the sediment and they reflect the chemistry of their source rocks (Rollinson 1993). La/Sc, Sc/Th, Co/Th, Zr/Hf, and Th/U ratios of immobile elements are also used to determine parent materials (McLennan & Taylor 1983; Taylor & McLennan 1985). In particular, the Nd/Sm ratio is an indicator of similarity and difference of source materials (Banner *et al.* 1988). Similar ratios of these

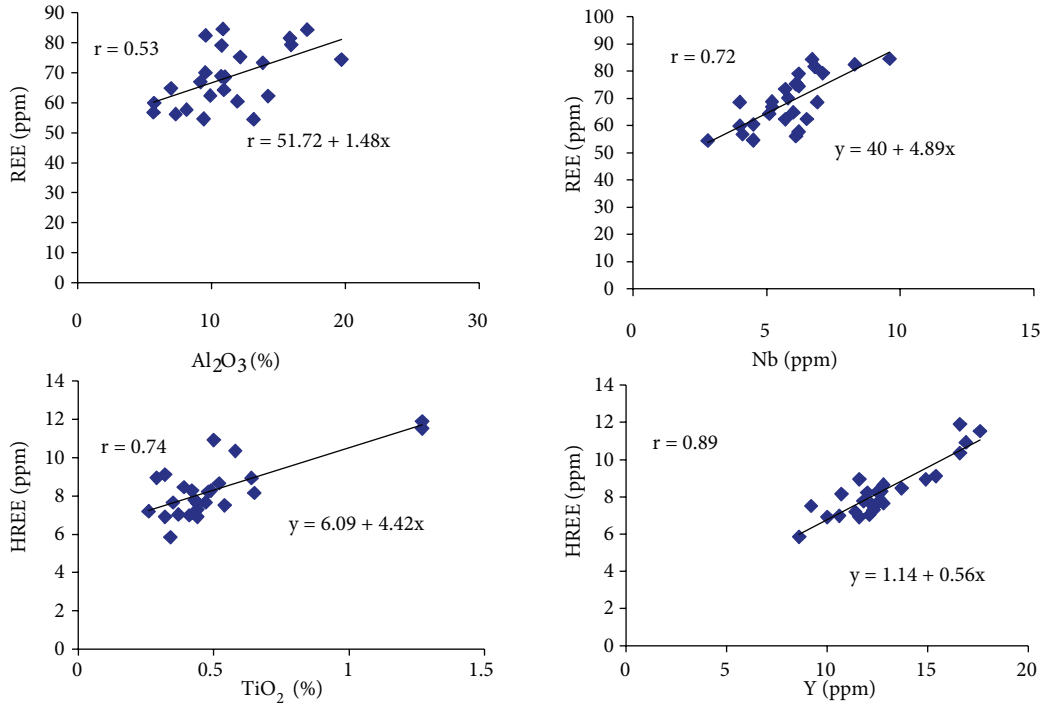


Figure 11. Some representative correlations between REEs and major and trace elements (the significance level is $\alpha = 0.05$ for correlation coefficient r).

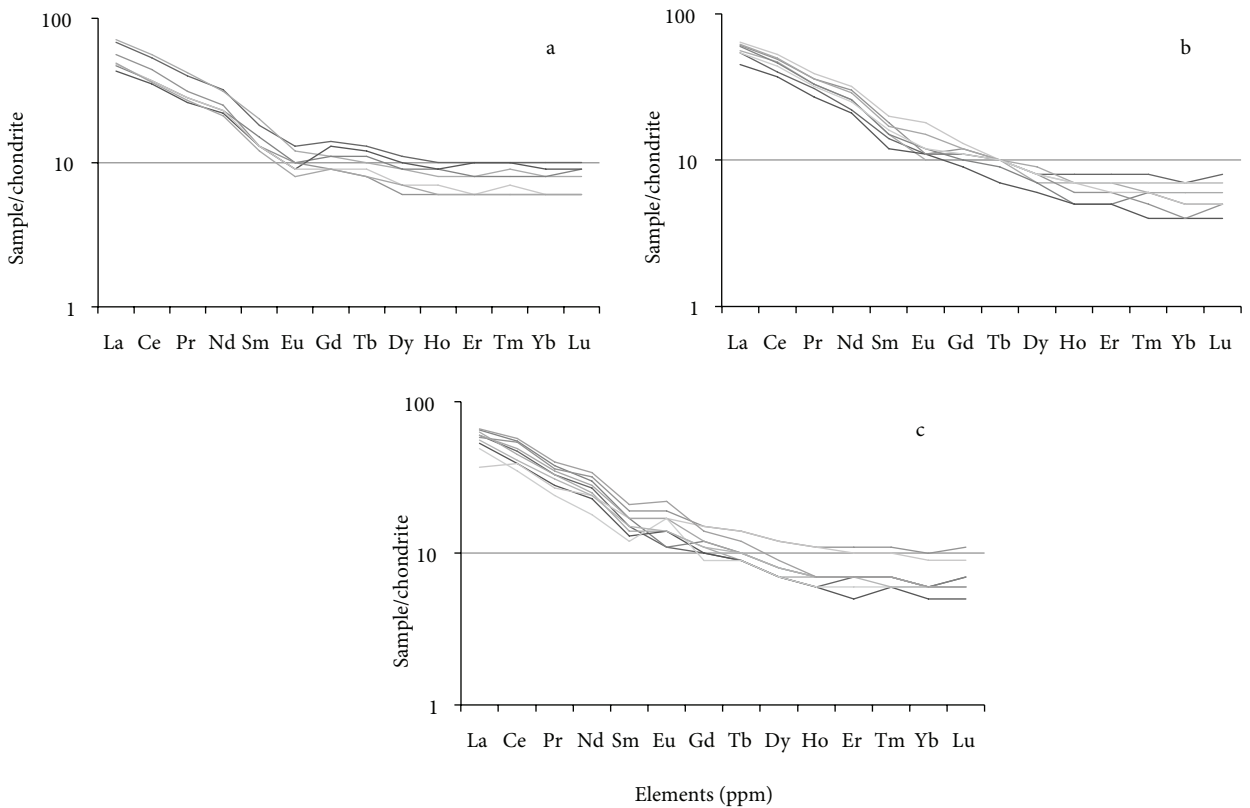


Figure 12. Chondrite-normalized REE patterns of (a) Akk, (b) Alt and (c) Ymt samples (data after Sun & McDonough 1989).

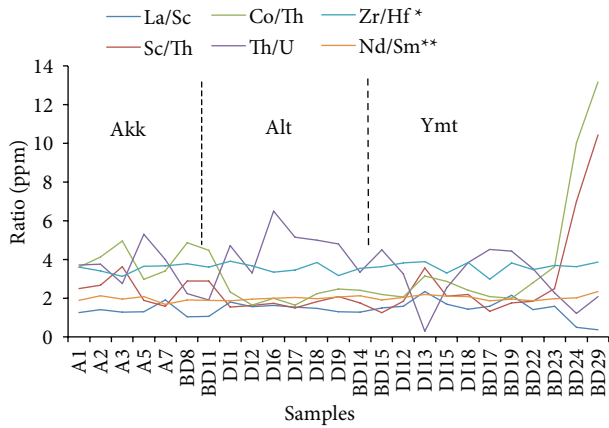


Figure 13. La/Sc, Sc/Th, Co/Th, Th/U, Zr/Hf, and Nd/Sm ratios in marine samples (Akk, Alt) and lacustrine samples (Ymt). Zr/Hf*: Zr/Hf / 10, Nd/Sm**: Nd/Sm × 10.

elements in Akk, Alt, and Ymt samples might imply that these rocks might have a common source (Figure 13).

The immobile elements such as Sc and Co are more concentrated in basic rocks than in felsic rocks, and Th is more abundant in felsic rocks (Taylor & McLennan 1985; Condie & Wronkiewicz 1990). The Sc/Th and Co/Th ratios of samples BD24–BD29 from lacustrine sediments are significantly high and their high Fe₂O₃ contents (8.46% and 10.29%, respectively) reflect the contribution of a basaltic component (Table 2; Figure 13).

Enrichment or depletion of LREEs and HREEs was quantified by the ratio of (La)_N/(Yb)_N. The average (La)_N/(Yb)_N (N: chondrite normalized; Sun & McDonough 1989) ratio is similar for the 3 rock types, indicating geochemical and mineralogical similarities of these groups. The (La)_N/(Yb)_N ratio decreases from acidic to basic types of rocks (Taylor & McLennan 1985). As expected, the (La)_N/(Yb)_N ratios of the 2 Ymt samples that have detrital basaltic rock fragments are lower (Figure 14).

One-way ANOVA was used to compare the 3 groups of (La)_N/(Yb)_N ratios by testing whether 2 or more populations means are equal (Noruois 2004). Statistical data showed that there were no significant differences ($F = 3.494$; Sig. = 0.048) at a level lower than the significance level of 0.05 among the Akk, Alt and Ymt samples.

6. Conclusions

Tuffite levels of the Alibonca Formation (Alt samples) and Yamadağ volcanites (Ymt samples) show similar optic microscopic features, except for the observation of basaltic rock fragments in Ymt samples. In SEM studies, similar assemblages were observed in Alt and Ymt samples, including authigenic smectite formation.

In Akk samples, clay minerals are not different from Alt and Ymt samples, which are composed in the order

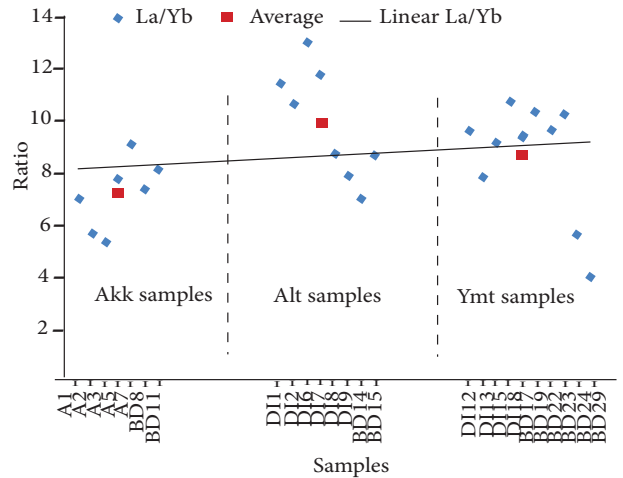


Figure 14. Average (La)_N/(Yb)_N (N: chondrite normalized, data after Sun and McDonough 1989) ratio of marine samples (Akk, Alt) and lacustrine samples (Ymt).

of smectite, palygorskite, illite, and S-C. Ca-smectite is the most dominant mineral in these 3 rock groups. Pyrite and coal occurrences, which are indicative of reducing conditions, are present only in Ymt samples.

Element ratios of Akk, Alt, and Ymt samples are quite similar. Both tuffites of marine and lacustrine units are quite similar in terms of bulk, clay, and trace element composition, suggesting that these deposits have a common source. In previous geologic and stratigraphic studies, due to similar appearance of tuffites in middle levels of the Alibonca Formation and Yamadağ Volcanites, the volcanism in the study area was proposed to be of Lower Miocene age. However, in the present work the mineralogy and geochemistry of lithostratigraphic units are also concluded to be similar, which, in turn, supports the idea that the volcanism was started in the lower Miocene. Consistent with recent interpretation of regional geologic history, we conclude that volcanism might have commenced in the Lower Miocene.

Acknowledgments

We are grateful to Professor Warren D Huff, PhD, University of Cincinnati, Ohio (USA), and Professor George E Christidis, PhD, Technical University of Crete, Department of Mineral Resources Engineering, (Greece), for their encouragement and editorial help. Special thanks go to Professor Hüseyin Yalçın, PhD, Cumhuriyet University, Sivas (Turkey), whose helpful reviews of the manuscript have greatly improved it. The financial support of the Firat University (Turkey) scientific research projects unit under FUBAP Project Number 2088 is gratefully acknowledged.

References

- Abdioğlu, E. & Arslan, M. 2005. Mineralogy, geochemistry and genesis of bentonites of the Ordu area, NE Turkey. *Clay Minerals* **40**, 131–151.
- Alpaslan, M. & Terzioğlu, N. 1996. Comparative geochemical features of the Upper Miocene and Pliocene volcanics around Arguvan (NW Malatya). *Geological Bulletin of Turkey* **39**, 75–86.
- Banner, J.L., Hanson, G.N. & Meyers, W.J. 1988. Rare earth element and Nd isotopic variations in regionally extensive dolomites from the Burlington-Keokuk Formation (Mississippian): implications for REE mobility during carbonate diagenesis. *Journal of Sedimentary Petrology* **58**, 415–432.
- Bauluz, B., Mayayo, M.J., Fernandez-Nieto, C. & Gonzalez Lopez, J.M. 2000. Geochemistry of Precambrian and Paleozoic siliciclastic rocks from the Iberian Range (NE Spain): implications for source-area weathering, sorting, provenance, and tectonic setting. *Chemical Geology* **168**, 135–150.
- Brindley, G.W. 1980. *Crystal Structures of Clay Minerals and their X-ray Identification*. Mineralogical Society, London.
- Brindley, G.W. 1981. Long-spacing organics for calibrating long spacings of interstratified clay mineral. *Clays & Clay Minerals* **29**, 67–68.
- Buket, E. & Temel, A. 1998. Major element, trace element, and Sr–Nd isotopic geochemistry and genesis of Varto (Muş) volcanic rocks, eastern Turkey. *Journal of Volcanological and Geothermal Research* **85**, 405–421.
- Çelik, M., Karakaya, N. & Temel, A. 1999. Clay minerals in hydrothermally altered volcanic rocks, Eastern Pontides, Turkey. *Clays and Clay Minerals* **47**, 708–717.
- Chamley, H. 1989. *Clay Sedimentology*. Springer-Verlag, Berlin.
- Christidis, G.E. 1998. Comparative study of the mobility of major and trace elements during alteration of an andesite and a rhyolite to bentonite, in the islands of Milos and Kimolos, Aegean, Greece. *Clays and Clay Minerals* **46**, 379–399.
- Christidis, G.E. 2001. Formation and growth of smectites in bentonites: a case study from Kimolos Island, Aegean, Greece. *Clays and Clay Minerals* **49**, 204–215.
- Christidis, G.E. & Huff, W.D. 2009. Geological aspects and genesis of bentonites. *Elements* **5**, 93–98.
- Christidis, G.E., Scott, R.W. & Marcopoulos, T. 1995. Origin of the bentonite deposits of Eastern Milts, Aegean, Greece: geological, mineralogical and geochemical evidence. *Clays and Clay Minerals* **43**, 63–77.
- Condie, K.C. 1993. Chemical composition and evolution of the upper continental crust: contrasting results from surface samples and shales. *Chemical Geology* **104**, 1–37.
- Condie, K.C. & Wronkiewicz, D.J. 1990. The Cr/Th ratio in Precambrian pelites from the Kaapvaal Craton as index of Craton evolution. *Earth and Planetary Science Letters* **97**, 256–267.
- Dalai, T.K., Rengarajan, R. & Patel, P.P. 2004. Sediment geochemistry of the Yamuna River System in the Himalaya: implications to weathering and transport. *Geochemical Journal* **38**, 441–453.
- Das, B.K. & Gaye-Haake, B. 2003. Geochemistry of Rewalsar Lake sediment, Lesser Himalaya, India: implications for source-area weathering, provenance and tectonic setting. *Geosciences Journal* **7**, 299–312.
- Debaar, H.J.W., Bacon M.P., Brewer P.G. & Bruland K.W. 1985. Rare earth elements in the Pacific and Atlantic Oceans. *Geochimica et Cosmochimica Acta* **49**, 1943–1959.
- Ece, Ö.I. & Nakagawa, Z. 2003. Alteration of volcanic rocks and genesis of kaolin deposits in the Şile Region, northern Istanbul, Turkey. Part II: differential mobility of elements. *Clay Minerals* **38**, 529–550.
- Ece, Ö.I. Schroeder Smilley, M.J. & Wampler, J.M. 2008. Acid-sulphate hydrothermal alteration of andesitic tuffs and genesis of halloysite and alunite deposits in the Biga Peninsula, Turkey. *Clay Minerals* **43**, 281–315.
- Ekici, T. 2003. *Petrology of the Neogene Volcanics Along the Malatya Fault Between Arguvan and Arapkir (Malatya)*. PhD Thesis. Çukurova University, Adana-Turkey [unpublished].
- Ekici, T., Alpaslan, M., Parlak, O. & Uçurum, A. 2009. Geochemistry of the Middle Miocene Collision-related Yamadağı (Eastern Anatolia) calc-alkaline volcanics, Turkey. *Turkish Journal of Earth Sciences* **18**, 511–528.
- Ercan, T. & Asutay, H.J. 1993. Petrology of Neogene-Quaternary volcanics around Malatya-Elazığ-Tunceli-Bingöl-Diyarbakır. *A. Suat Erk Geology Symposium*, Ankara, 291–302 [in Turkish with English abstract].
- Erkoyun, H. & Kadir, S. 2011. Mineralogy, micromorphology, geochemistry and genesis of a hydrothermal kaolinite deposit and altered Miocene host volcanites in the Hallaçlar area, Uşak, western Turkey. *Clay Minerals* **46**, 421–448.
- Gündoğdu, N. 1982. *Geological-Mineralogical and Geochemical Investigation of Neogene-Bigadiç Sedimentary Basin*. PhD Thesis. Hacettepe University, Ankara-Turkey [unpublished, in Turkish with English abstract].
- Glassman, J.R. 1982. Alteration of andesite in wet, unstable soils of Oregon's Western Cascades. *Clays and Minerals* **30**, 253–263.
- Hover, V. & Ashley G.M. 2003. Geochemical signatures of paleodepositional and diagenetic environments: a STEM/AEM study of authigenic clay minerals from an arid rift basin, Olduvai Gorge, Tanzania. *Clays and Clay Minerals* **51**, 231–251.
- Huff, W.D. 2006. Volcanism and its contribution to mudrock genesis. *Turkish Journal of Earth Sciences* **15**, 111–122.
- Huggenberg, H. & Fuchtbauer, H. 1988. Clay minerals and their diagenesis in carbonate-rich sediments. *Proceedings of the Ocean Drilling Program, Scientific Results* **101**, 171–177.
- Innocenti, F., Mazzuoli, R., Pasquare, G., Radiati di Brozola, F. & Villari, L. 1976. Evolution of volcanism in the area of interaction between the Arabian, Anatolian and Iranian plates (Lake Van, Eastern Turkey). *Journal of Volcanology and Geothermal Research* **1**, 103–112.
- Kadir, S. & Akbulut, A. 2009. Mineralogy, geochemistry and genesis of the Taşoluk kaolinite deposits in pre-Early Cambrian metamorphites and Neogene volcanites of Afyonkarahisar, Turkey. *Clay Minerals* **44**, 89–112.

- Kadir, S. & Erkoyun, S. 2012. Genesis of the hydrothermal Karacayır kaolinite deposit in Miocene Volcanics and Palaeozoic metamorphic rocks of the Uşak-Güre Basin, Western Turkey. *Turkish Journal of Earth Sciences* **21**, 1–26.
- Kamineneni, D.C. 1985. Significance of the distribution of rare-earth elements (REE) in the Eye-Dashwa pluton the migration of radionuclides. *Atomic Energy of Canada Limited Technical Record* **113**, 508–527.
- Karakaya, M.Ç., Karakaya, N. & Küpeli, Ş. 2011. Mineralogical and Geochemical properties of the Na- and Ca-Bentonites of Ordu (N.E. Turkey). *Clays and Clay Minerals* **59/1**, 75–94.
- Karakaya, M.Ç., Karakaya, N. & Temel, A. 2001. Kaolin occurrences in the Erenler Dağı volcanics, southwest Konya Province, Turkey. *International Geology Review* **43**, 711–721.
- Karakaya, N. 2009. REE and HFS element behaviour in the alteration facies of the Erenler Dağı Volcanics (Konya, Turkey) and kaolinite occurrence. *Journal of Geochemical Exploration* **101**, 185–208.
- Karakaya, N., Karakaya, M.Ç. & Temel, A. 2011. Mineralogical and geochemical characteristics and genesis of the sepiolite deposits at Polatlı Basin (Ankara, Turkey). *Clays and Clay Minerals* **59/3**, 286–314.
- Keskin, M., Pearce, J.A. & Mitchell, J.G. 1998. Volcano-stratigraphy and geochemistry of collision-related volcanism on the Erzurum-Kars Plateau, Northern Turkey. *Journal of Volcanology and Geothermal Research* **85**, 355–404.
- Křibek, B., Strnad, M., Boháček, Z., Sýkorová, I., Čejka, J. & Sobalik, Z. 1998. Geochemistry of Miocene lacustrine sediments from the Sokolov Coal Basin (Czech Republic). *International Journal of Coal Geology* **37**, 207–233.
- Kürüm, S., Akgül, B. & Erdem, E. 2006. Examples of Neogene volcanism in Eastern Turkey: comparative petrographic, geochemical and petrologic features of Malatya–Elazığ–Tunceli volcanics. *Journal of the Geological Society of India* **68**, 129–136.
- Leo, D.P., Dinelli, E., Mongelli, G. & Schiattarella, M. 2002. Geology and geochemistry of Jurassic pelagic sediments, Scisti Silicee Formation, Southern Apennines, Italy. *Sedimentary Geology* **150**, 229–246.
- Leo, W.G., Marvin, R.F. & Menhert, H.H. 1974. Geological framework of the Kuluncak-Sofular area, East-Central Turkey and K-Ar ages of igneous rocks. *Geological Society of America Bulletin* **85**, 1785–1788.
- Lopez, J.M.G., Bauluz, B., Fernandez-Nieto, C., Yuste Oliete, A. 2005. Factors controlling the trace-element distribution in fine-grained rocks: the Albia kaolinite-rich deposits of the Oliete Basin (NE Spain). *Chemical Geology* **214**, 1–19.
- McLennan, S.M. & Taylor, S.R. 1983. Geochemical evolution of the Archean shales from South Africa. I. The Swaziland and Pongola supergroups. *Precambrian Research* **22**, 93–124.
- Middelburg, J.J., Van Der Weijden, C.H. & Woittiez, J.R.W. 1988. Chemical processes affecting the mobility of major, minor and trace elements during weathering of granitic rocks. *Chemical Geology* **68**, 253–273.
- Mongelli, G. 1997. Ce-anomalies in the textural components of upper Cretaceous karst bauxites from the Apulian carbonate platform (southern Italy). *Chemical Geology* **140**, 69–79.
- Nance, W.B. & Taylor, S.R. 1976. Rare earth element patterns and crustal evolution Australian post-Archean sedimentary rocks. *Geochimica et Cosmochimica Acta* **40**, 1539–1551.
- Nesbitt, H.W. 1979. Mobility and fractionation of REE during weathering of granodiorite. *Nature* **279**, 206–210.
- Noruöis, M.J. 2004. *SPSS 12.0 Guide to Data Analysis*. Prentice Hall, New Jersey.
- Ortega-Huertas, M., Martinez-Ruiz, F., Palomo, I. & Chamley, H. 2002. Review of the mineralogy of the Cretaceous–Tertiary boundary clay: evidence supporting a major extraterrestrial catastrophic event. *Clay Minerals* **37**, 395–411.
- Perinçek, D. 1979. *The Geology of Hazro-Korudag-Çüngüs-Maden-Ergani-Hazar-Elazığ-Malatya Area*, Geological Congress of Turkey, Ankara.
- Plank, T. & Langmuir, C.H. 1998. The chemical composition of subducting sediment and its consequences for the crust and mantle. *Chemical Geology* **145**, 325–394.
- Rashid, S.A. 2002. Geochemical characteristics of Mesoproterozoic clastic sedimentary rocks from the Chakrata Formation, Lesser Himalaya: implications for crustal evolution and weathering history in the Himalaya. *Journal of Asian Earth Sciences* **21**, 283–293.
- Rollinson, H.R. 1993. *Using Geochemical Data: Evaluation, Presentation, Interpretation*. Longman, Essex, UK.
- Saleemi, A.A. & Ahmed, Z. 2000. Mineral and chemical composition of Karak mudstone, Kohat Plateau, Pakistan: implications for smectite-illitization and provenance. *Sedimentary Geology* **130**, 229–247.
- Şaroğlu, F. & Yılmaz, Y. 1986. Geological evolution and basin models during the neotectonic episode in Eastern Anatolia. *Mineral Research & Exploration Institute of Turkey* **107**, 61–83.
- Şengör, A.M.C., Görür, N. & Şaroğlu, F. 1985. Strike-slip faulting and related basin formation in zones of tectonic escape: Turkey as a case study. In: Biddle, K.T. & Christie-Blick, N. (eds), *Strike-slip Deformation, Basin Formation and Sedimentation*. Society of Economic Mineralogist and Paleontologists Special Publications **37**, 227–264.
- Shibata, S., Tanaka, T. & Yamamoto, K. 2006. Crystal structure control of the dissolution of rare earth elements in water-mineral interactions. *Geochemical Journal* **40**, 437–446.
- Shoval, S. 2004. Clay sedimentation along the southeastern Neo-Tethys margin during the oceanic convergence stage. *Applied Clay Science* **24**, 287–298.
- Spears, D.A., Kanaris-Sotirios, R., Riley, N. & Krause, P. 1999. Namurian bentonites in the Pennine basin, UK-origin and magmatic affinities. *Sedimentology* **46**, 385–401.
- Sun, S.S. & McDonough, W.F. 1989. Chemical and isotopic systematics of oceanic basalts; implications for mantle composition and processes. In: Saunders, A.D. & Norry, M.J. (eds), *Magmatism in the Ocean Basins*. Geological Society of London, London, **42**, 313–345.

- Tandon, S.K. 2002. Records of the influence of volcanism on contemporary sedimentary environments in central India. *Sedimentary Geology* **147**, 177–192.
- Taylor, S.R. & McLennan, S.H. 1985. *The Continental Crust: Its Composition and Evolution*. Blackwell, Oxford.
- Turan, M. 1984. *The Stratigraphy and Tectonics of Baskil-Aydınlı (West of Elazığ, E. Turkey) Area*. PhD Thesis. Fırat University, Elazığ-Turkey [unpublished].
- Türkmen, Aksoy, E., Kürüm, S., Akgül, B. & İnceöz, M. 1998. Lower Miocene volcanism of Arguvan-Arapgir (Malatya) region and their significance in the regional stratigraphy. *Geosound* **32**, 103–115.
- Winchester, J.A. & Floyd, P.A. 1977. Geochemical discrimination of different magma series and their differentiation products using immobile elements. *Chemical Geology* **20**, 325–43.
- Worash, G. & Valera, R. 2002. Rare earth element geochemistry of the Antalo Supersequence in the Mekele Outlier (Tigray region, northern Ethiopia). *Chemical Geology* **182**, 395–407.
- Velde, B. 1995. *Origin and Mineralogy of Clays*. Springer, Berlin.
- Yalçın, H. & Bozkaya, Ö. 2002. Alteration mineralogy and geochemistry of the Upper Cretaceous Volcanics around Hekimhan (Malatya), central east Turkey: an example for the seawater-rock interaction. *Bulletin of Faculty of Engineering of Cumhuriyet University, Series A Earth Sciences* **19/1**, 81–98 [in Turkish with English abstract].
- Yalçın, H. & Gümüşer, G. 2000. Mineralogical and geochemical characteristics of Late Cretaceous bentonite deposits at the north of Kelkit valley, Northern Turkey. *Clay Minerals* **35**, 807–825.
- Yalçın, H., Gündoğdu, M.N., Gaugoud, A., Vidal, P. & Uçurum, A. 1998. Geochemical characteristics of Yamadağı volcanics in Central East Anatolia: an example from collision-zone volcanism. *Journal of Volcanology Geothermal Research* **85**, 303–326.
- Yıldız, A. & Kuşcu, M. 2007. Mineralogy, chemistry and physical properties of bentonites from Başören, Kütahya, W Anatolia, Turkey. *Clay Minerals* **42**, 399–414.
- Yılmaz, Y., Güner, Y. & Şaroğlu, F. 1998. Geology of the Quaternary volcanic centres of the east Anatolia. *Journal of Volcanology and Geothermal Research* **85**, 173–210.